International Journal of Ecology and Environmental Sciences 49: 481-488, 2023
ISSN: 2320-5199 (Online); https://doi.org/10.55863/ijees.2023.2802

Assessment of Land Surface Temperature in Relation to Built-up Index: A Case Study on Nagaon District, Assam, India

RIMLEE BORA
Department of Geography, Gauhati University, Assam, India
E-mail: borarimlee@gmail.com

ABSTRACT
When calculating the surface temperature from thermal data, the Land Surface Temperature (LST) is an essential statistic. The goal of this research is to use multi-temporal data to capture the time-space contrast of land surface temperature in the Nagaon district of Assam, as well as the relationship between land surface temperature and the built-up index. Ratio of Variation to the mean Normalized Difference Built-up Index (NDBI) employs the infrared spectrum to evaluate man-made urban environments. Three sets of satellite images spanning three decades (1992, 2004, and 2021) are imported into ArcGIS, where spatial-temporal LST data is extracted using the mono window algorithm approach, and the resulting dataset is examined statistically and cartographically. The findings denote that maximum and minimum temperatures have been rising during the period of 1992-2021. LST increases 2.77ºC in terms of minimum temperature from 1992 to 2004 and 1.93ºC rises from 2004 to 2021.The Pearson correlation approach has been applied to the question of how LST relates to NDBI. The present study demonstrated that LST and NDBI have strong reciprocity (R^2=0.867, 0.854, 0.947 for 1992, 2004 and 2021, respectively). Since the built-up area can be easily accessed from both NDBI and LST, this suggests that it is a large contributor to the urban heat island effect.

Key words: Land Surface Temperature, Infra-red band, Spatio-temporal, Normalized Difference Built-up Index, Mono Window Algorithm, Urban Heat Island.

INTRODUCTION

The greatest hazard that civilization faces right now is an increase in global surface temperatures caused by the replacement of green areas with impermeable ones. The temperature at the interface between the ground and the air is known as the land surface temperature. Land Surface Temperature (LST) is an accurate proxy for average temperatures around the world and in specific regions. LST influences climate, which in turn influences surface activity, but it also, influences the relationship between sensible and latent heat flow. Numerous fields make use of LST data, including evapotranspiration, atmospheric phenomena, and global water circulation, observation of vegetation and urban climate, and ecological study (Aires et al. 2001, Sun et al. 2004). Atmospheric releasing heat from the ground determines the LST (Bastiaanssen et al.1998, Weng 2009), which in turn controls the interplay of heat and moisture at the atmosphere's farthest edges. In many studies on urban heat islands have relied on air and ground temperature monitoring. A variety of land use and land cover surfaces can be monitored for temperatures using LST data. It is widely used for checking and predicting harvests in the agriculture sector (Shukla 2018). The impact of LULC on Urban Heat Island (UHI) effect has also been studied with Normalized Difference Built-up Index (NDBI) and Nortmalized Difference Vegetation Index (NDVI).

When used for data gathering and analysis, remote sensing provides precise geographical information at low cost, yielding more reliable results. This enables a first-of-its-kind global study of LST. There is an automatic connection between the LST and satellite thermal infrared (TIR) data. LST can also be used to detect changes in land use/cover, urbanization, and desertification (Lein 2011). The pace of surface heating influences the amount of LST that rises, and this is a major factor in the overall climatic changes that result from urbanization. There are a number of methods for regaining LST, one of which is the Radiative Transfer Equation (RTE) technique (Hasnat 2019), Single Channel algorithm (Weng 2009) and Mono Window algorithm method (Hasnat 2019). In this work, Landsat 5 and 8 images are processed with the Mono Window Algorithm (MWA) method, where single thermal band is used. NDBI occurs when Short Wave Infra Red reflectance

is higher than Near Infra Red reflectance, and it is useful for locating urban areas. The NDBI is compatible with both Landsat TM's spectral band 5 and 4.

The objectives of this study are to understand the geographical and temporal dynamics of land surface temperature and urbanization and to analyse the association between the two.

MATERIAL AND METHODS

Study area

Nagaon District is located in the southern bank of river Brahmaputra. The area extends between 25º45' and 26º45' N latitude and 91º50' and 93º20' E longitude. The Brahmaputra River forms its northern border; Karbi Anglong and Golaghat districts form its eastern and western borders; and the districts of West Karbi Anglong, Hojai, and Dima Hasao form its southern borders (Fig. 1). The population is 1892550 persons and total area 2929 km^2 (Census 2011).

Database and methodology

The study made use of multispectral satellite images of 1992, 2004 and 2021 from the United States Geological Survey (USGS) archive (Table 1). Landsat series images revealed spatial and temporal changes in the study area's land surface temperature and built-up area. ArcGIS software was used to analyse the satellite data and visualize the outputs.

Normalized Difference Built-up Index (NDBI)

The Normalized Difference Built-up Index (NDBI) highlights artificial built-up areas by using the Near Infra Red (NIR) and Mid Infra Red (MIR) bands (Zha et al. 2003). NDBI is expressed as follows

$$NDBI = \frac{MIR - NIR}{MIR + NIR} \quad \ldots\ldots\ldots\ldots\ldots\ldots\ldots\ldots\ldots\ldots\ldots\ldots (1)$$

Band 4 is near-infrared and band 5 is mid-infrared reflectance in Landsat 5 thematic mapper images.

Table: 1 Characteristics of Satellite Data

Satellite	Sensor	Year of acquisition	Path/Row	Resolution
Landsat 5	Thematic Mapper(TM)	1992/05/10	136/42	30m
Landsat 5	Thematic Mapper(TM)	2004/05/11	136/42	30m
Landsat 8	Operational land Imager(OLI) and Thermal Infrared Sensor(TIRS)	2021/05/13	136/42	30m

Source: USGS earth explorer

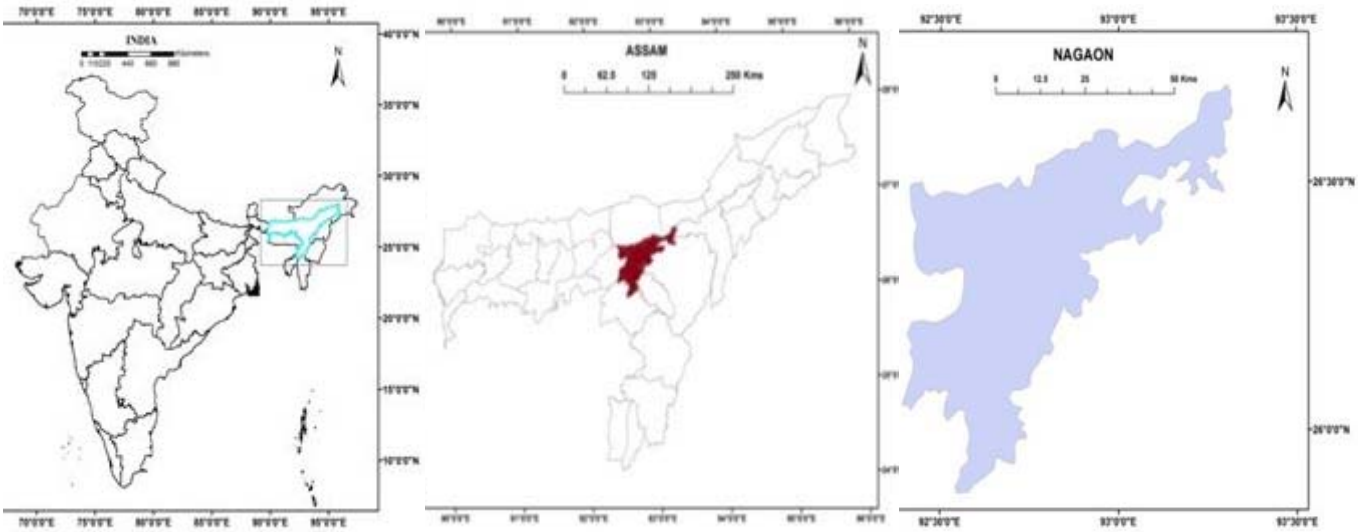

Figure 1: Locational map of the study area

Band 5 is for Near-Infrared and Band 6 is the Mid-Infrared for Landsat 8 images. The value of NDBI can vary from -1 to 1, with higher values indicating highly developed built-up land and bigger developable land areas.

Calculation of Land Surface Temperature (LST)

Conversion of digital numbers to top of atmospheric (TOA) reflectance

For Landsat 5, band 6 is converted into top of atmospheric reflectance using following equation

$$L\lambda = \frac{LMAX\lambda - LMIN\lambda}{QCALMAX - QCALMIN} x(QCAL - QCALMIN) + LMIN\lambda \quad (2)$$

where Lλ= Spectral Radiance, QCAL = Quantized calibrated pixel value in DN, LMAXλ= Spectral radiance scaled to QCALMAX in [Watts/ (m^2 _ sr _ mm)], LMINλ= Spectral radiance scaled to QCALMIN in [Watts/(m^2_sr_mm)], QCALMIN = Minimum quantized calibrated pixel value (corresponding to LMINë) in DN, QCALMAX = Maximum quantized calibrated pixel value (corresponding to LMAXλ) in DN = 255.

For Landsat 8, band 10 is converted into top of atmospheric reflectance value with the help of following value,

$$L\lambda = ML\ x\ QCAL + AL - Oi \quad (3)$$

where Lλ = Top of atmosphere spectral radiance [Watts/(m^2_sr_mm)], ML = Radiance multiplicative Band (No.), AL = Radiance Add Band (No.), Qcal = Quantized and calibrated standard product pixel values (DN), Oi = correction value for Band 10 is 0.29.

Conversion of Top of Atmospheric reflectance to Brightness Temperature (BT)

Top of atmospheric value is converted to brightness temperature using following equation

$$BT = \frac{K2}{\ln(\frac{K1}{L\lambda}+1)} - 273.15 \quad (4)$$

where BT = Top of atmosphere brightness temperature (ºC), Lλ = TOA spectral radiance [Watts/(m^2_sr_mm)], K1 and K2 are calibration constants (provided in metadata file).

Derivation of Normalized Difference Vegetation Index (NDVI)

The NDVI is used to define the abundance of vegetation in an area. The NDVI value ranges from -1 to 1. With more vegetation indicated a higher NDVI value and less vegetation indicated a lower NDVI value. The formula for calculating NDVI is For Landsat 5,

$$NDVI = \frac{NIR(BAND\ 4) - RED(BAND\ 3)}{NIR\ (BAND\ 4) + RED(BAND\ 3)} \quad (5)$$

For Landsat 8,

$$NDVI = \frac{NIR(BAND\ 5) - RED(BAND\ 4)}{NIR\ (BAND\ 5) + RED(BAND\ 4)} \quad (6)$$

Land surface emissivity

With the help of NDVI value land surface emissivity can be calculated. The formula for calculating land surface emissivity is

$$Pv = \left(\frac{NDVI - NDVImin}{NDVImax - NDVImin}\right)^2 \quad (7)$$

where Pv = Proportion of Vegetation, NDVI = DN values from NDVI Image, NDVI min = Minimum DN values from NDVI Image, NDVI max = Maximum DN values from NDVI Image.

$$\varepsilon = \varepsilon s(1 - pv) + Ev\ x\ Pv \quad (8)$$

where • = Land Surface Emissivity, Pv = Proportion of Vegetation

Derivation Land Surface Temperature (LST)

LST can be measured using thermal band. It is used to measure temperature of land and thermal emissivity. The formula for calculating LST is

$$LST = \frac{BT}{1 + \left(\lambda\ x \frac{BT}{C2}\right) x \ln(E)} \quad (9)$$

where λ= wavelength of emitted radiance in ìm, c2= hc/s (h=Planck's constant, s=Boltzmann constant, c=velocity of light in m/s)cvn.

The flow chart of the methodology used is given in Figure 2.

RESULTS AND DISCUSSION

Spatio-temporal variation in LST

LST maps for three years (1992, 2004, and 2021) showed temporal and spatial patterns of LST concentration which imply the changing land use pattern for the study area. The range of temperature was 10.89-19.37ºC and mean LST 15.13ºC for the year 1992 (Fig. 3a). For the year 2004, the maximum temperature was 27.44ºC and minimum temperature 13.66ºc with mean LST 20.55ºC (Fig. 3b). Similarly, in 2021 the maximum and minimum temperature range was 33.42-15.59ºC and mean LST 24.50ºC

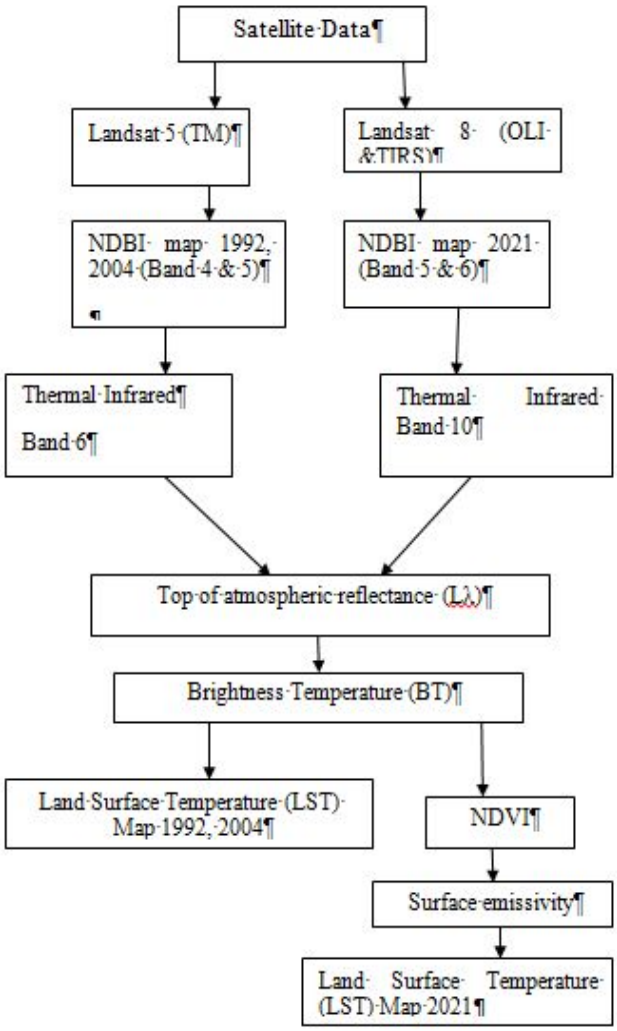

Figure 2: Methodological flowchart

(Fig. 3c).

LST values were categorized based on their range, and the area of each category was assessed. For LST range of 10.89-13.59ºC the area was 8.08% of the total area, followed by for 13.59-14.48ºC LST the area was 17.62%, for 14.48-15.15ºC LST the area was 36.56%, for 15.15-15.94ºC LST the area was 31.17% and for 15.94-19.37ºC the area was 6.57% for the year 1992. For LST range of 10.89-13.59ºC the area was 6.38% of the total area followed by for 13.59-14.48ºC LST the area was 22.21%, for 14.48-15.15ºC LST the area was 27.33%, for 15.15-15.94ºC LST the area was 31.55% and for 15.94-19.37ºC LST the area was 12.53% for the year 2004. For the LST range of 10.89-13.59ºC the area was 7.49% of the total area followed by for 13.59-14.48ºC LST the area was 16.39%, for 14.48-15.15ºc LST the area was 18.74%, for 15.15-15.94ºC LST the area was 27.75% and for 15.94-19.37ºC LST the area was 29.64% for the year 2021 (Table 3, Figs. 4, 5).

Spatio-temporal variation in NDBI

To calculate human-induced artificial land, the Built-up Index is exerted (Rahaman and Shermin 2021). The NDBI is as subservient index to ascertain the impact of land use on the environment (Yadav et al. 2019). The NDBI value ranges between -1 and 1. The value nearest to 1 indicates more built-up land,

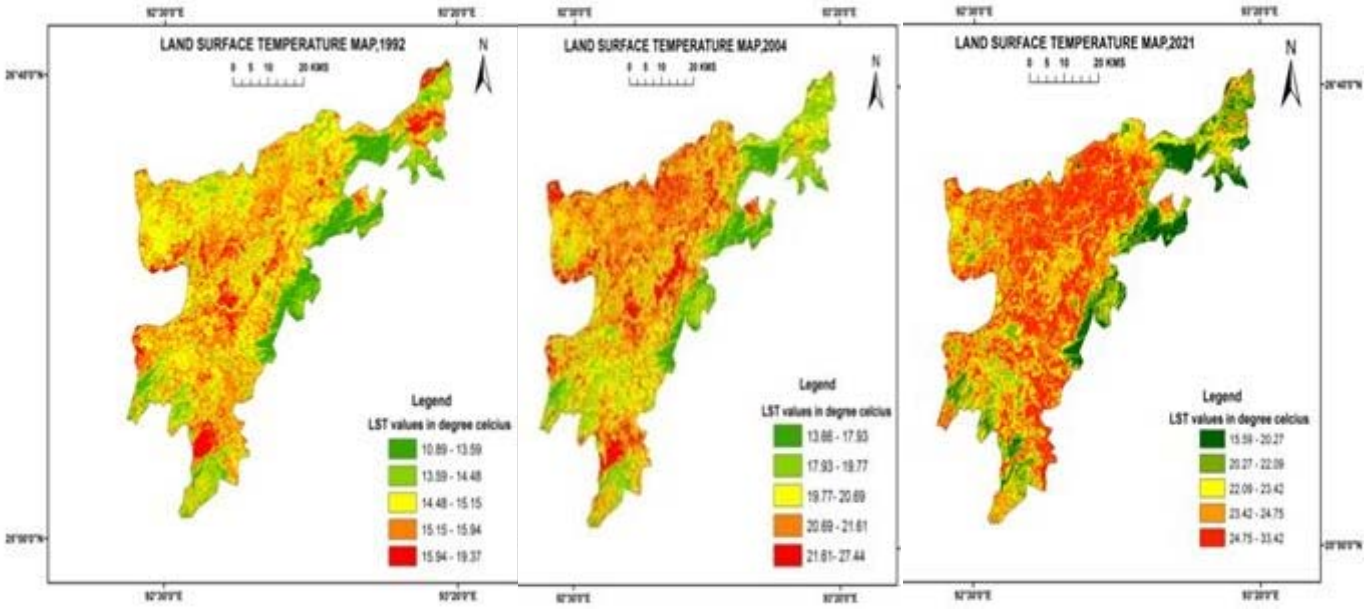

Figure 3. LST maps for 1992(a), 2004(b) and 2021(c)

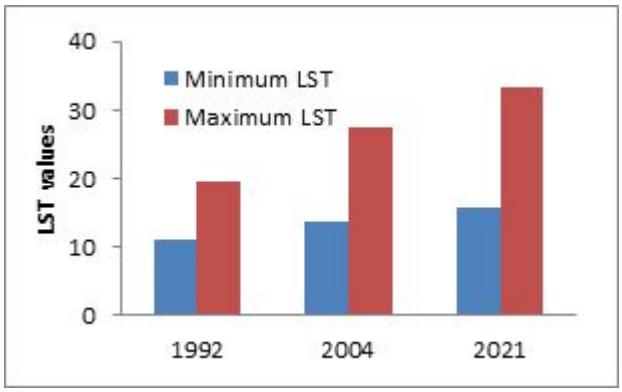

Figure 4. Maximum and Minimum LST values

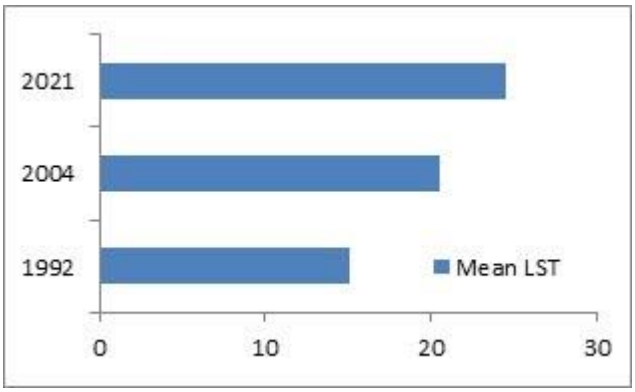

Figure 5: Mean LST variation

while the value nearer to -1 indicates less built-up land (Zha et al.2003). The NDBI varied between 0.275 to -0.153 in 1992. The maximum NDBI for the period 1992-2004 is 0.321, while the greatest NDBI for the period 2004-2021 is 0.054. The range of NDBI values is narrow in both scenarios. The changing NDBI values between 1992 and 2021 demonstrate how population growth impacts the demand for land, which in turn influences the built-up area (Table 4).

Table 3: Calculation of area on each LST category

LST range	1992		2004		2021		Net change in area	
	Area in km^2	%	Area in km^2	%	Area in km^2	%	1992-2004	2004-2021
10.89-13.59ºC	236.81	8.08	186.78	6.38	219.26	7.49	-0.21	0.17
13.59-14.48ºC	516.10	17.62	650.69	22.21	480.04	16.39	0.26	-0.26
14.48-15.15ºC	1070.88	36.56	800.48	27.33	548.99	18.74	-0.25	-0.31
15.15-15.94ºC	913.17	31.17	924.27	31.55	812.82	27.75	0.01	-0.12
15.94-19.37ºC	192.41	6.57	367.15	12.53	868.27	29.64	0.90	1.36

Table 4. Statistical results of NDBI values

Year	NDBI Values		Standard	Coefficient
	Maximum	Minimum	Deviation	of variation
1992	0.275	-0.153	0.14	5.13
2004	0.596	-0.147	0.17	5.34
2021	0.65	-0.014	0.19	5.58

Table 5. Correlation between LST and NDBI

Year	R^2
1992	0.867
2004	0.854
2021	0.947

NDBI and LST relationship

Inseparable ties connect the LST to the NDBI. There is a clear connection between the two factors. The LST was commonly used to represent land surface temperature changes. The rate at which the land surface heats up corresponds with the expansion of the urban zone. The NDBI-LST data shows that urban regions tend to be warmer than their rural counterparts. Consequently, urbanization has been hypothesized to result in significant variations in surface temperature.

In 1992, 2004, and 2021, the NDBI and LST were positively correlated (R^2=0.867, 0.854, and 0.947, respectively), indicating a strong positive relationship (Fig. 6, Table 5). This indicates that there is a positive correlation between LST and built-up area, and that urban areas benefit greatly from this factor in terms of heating.

This study's findings indicate that the built-up index is an important parameter for calculating the impact of human actions on changing land surface temperature patterns. The land's surface temperature was lower in 1992 than it will be in 2004 or 2021. The land surface temperature in the research area is

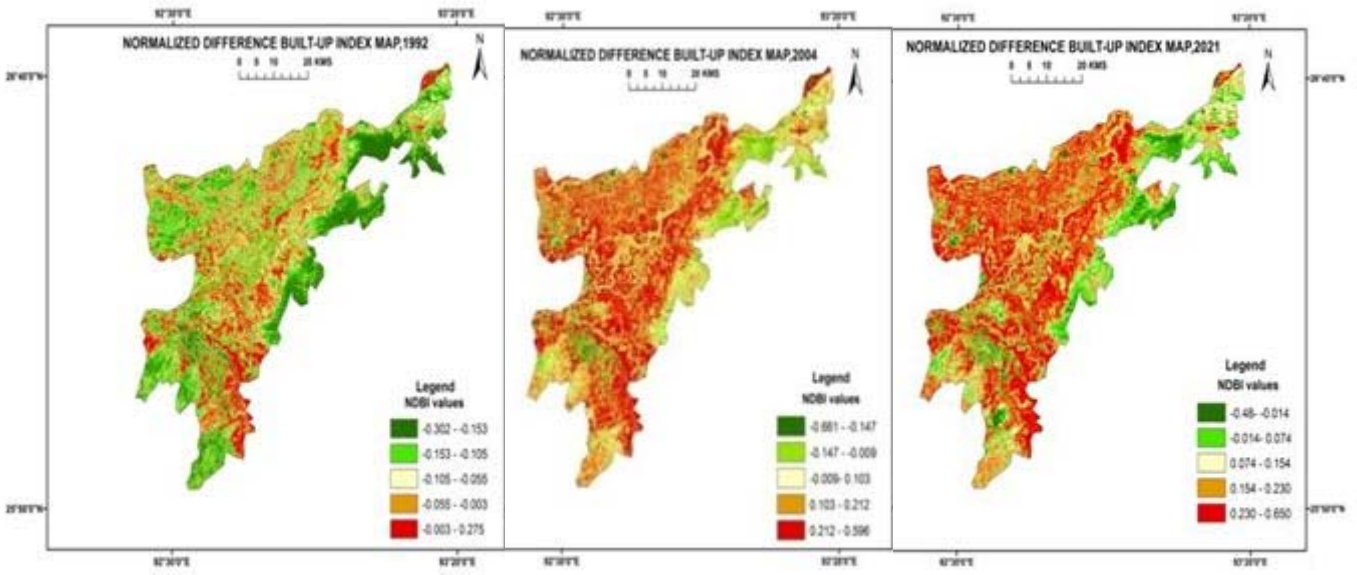

Figure 6: NDBI maps for 1992, 2004 and 2021

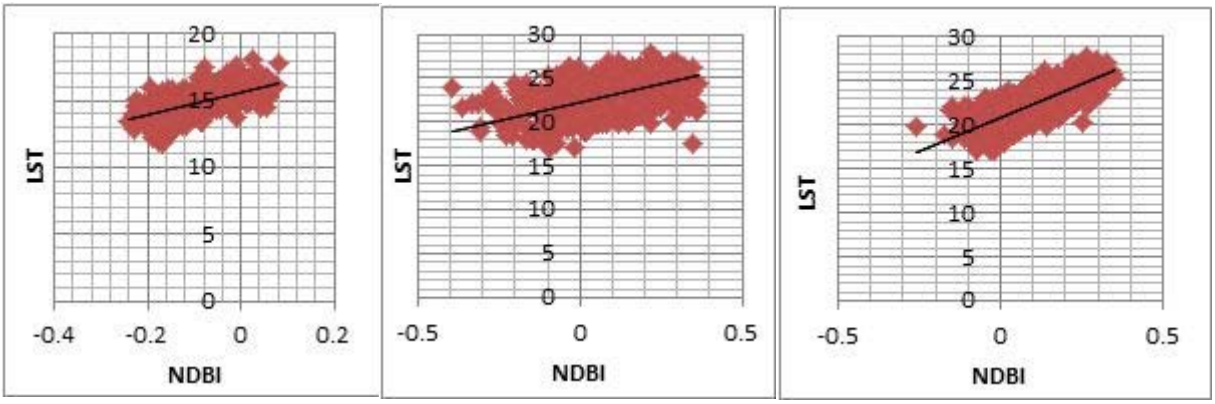

Figure 7. LST and NDBI relationship for 1992, 2004 and 2021

affected by the fewer of developed land and bare surface, as well as the significant amount of forest cover. In 2004, there was a marked rise in the land surface temperature. As forested land disappears, the urban footprint of the study region expands. Between 1992 and 2004, the area's temperatures went up. Minimum and maximum temperature differentials throughout this time are 8.07°C and 2.77°C, respectively. Changes in the LULC pattern and an increase in developed land have resulted in a reshuffling of forest cover in the study area. Therefore, the LST is increased. Vegetation, especially greenery, can serve to mitigate LST and cool the atmosphere. The greatest and minimum temperature variations throughout the period of 2004-2021 were 5.98 degrees and 1.93 degrees, respectively. The built-up area in the research area is influencing the temperature pattern, as evidenced by the variations in NDBI values. When considering the relationship between the environment and the atmosphere, LST is a critical point (Khandelwal et al. 2018). Multiple factors contribute to the observed increase in LST in the region under investigation. Land use change is a major contributor to the variability of LST over spatial and temporal scales. Population growth and land shortages have prompted a shift in how land is being used. Increases in land surface temperature can be attributed to a number of factors, including the growth of the built environment, the conversion of formerly undeveloped land into homes, and the intensification of agricultural land. However, the most significant

factor is the dramatic decline in forest cover in the region. The rate of urbanization is increasing. As a direct outcome of this process, many deforestation practices have been implemented. This has resulted in a decrease in the average annual rainfall.

CONCLUSIONS

The research was carried out to learn more about the land surface temperature and the urban expansion in the area from 1992 to 2021. All-year temperature increases at the surface are accompanied by LST that is more varied than in years past due to the orienting influence of already developed areas. According to the LST study, surface temperatures are higher in the urbanized and bare areas and lower in the well-vegetated regions. Based on satellite data from Band 6 and Band 5, 4, the NDBI provides a description of the urbanized landscape. In general, a greater amount of NDBI is associated with a greater amount of land area that is under construction. Positive correlations between NDBI and LST were observed. In addition to assessing and forecasting LST, NDBI may be used to display the UHI effect in any location, providing a solid basis for urban design and planning. The local ecosystem is threatened by human development and LST. Growth in LSTs could cause environmental changes that could endanger the health of people and other living things. Relocating people and goods from densely populated areas to the periphery can help bring down global temperatures. Therefore, various non-governmental and governmental groups should initiate reforestation programmes to lower the surface temperature, and the urban planning department should continue to enforce the urban land use management policy to limit wasteful use of land. The impacts of excessive heat can be mitigated by planting trees and shrubs, and by leaving open areas of land with a minimum of concrete structures.

ACKNOWLEDGMENT

Author acknowledges the support extended by the Department of Geography, Gauhati University for this research.

Conflict of Interest: The author declares no conflict of interest.

REFERENCES

Aires, F., Prigent, C., Rossow, W.B. and Rothstein, M. 2001. A new neural network approach including first guess for retrieval of atmospheric water vapor, cloud liquid water path, surface temperature, and emissivities over land from satellite microwave observations. Journal of Geophysical Research: Atmospheres, 106(D14), 14887–14907. https://doi.org/10.1029/ 2001jd900085

Bakhit, S. and Abdelkader, S. 2019. Assessment of urban growth patterns using spatio-temporal data and analysis. Asian Journal of Applied Sciences, 7(5), 546-556. https://doi:10.24203/ajas. v7i5.5975

Bastiaanssen, W., Menenti, M., Feddes, R. and Holtslag, A. 1998. A remote sensing surface energy balance algorithm for land (SEBAL). 1. Formulation. Journal of Hydrology, 212–213, 198–212. https://doi.org/10.1016/s0022-1694(98)00253-4

Das, G. and Dandapath, P. 2016. A spatio-temporal change analysis and assessment of the urban growth over Delhi National Capital Territory (NCT) during the period 1977-2014. International Journal of Experimental Research and Review, 7, 53-61.

Dong, J., Crow, W. and Bindlish, R. 2018. The error structure of the SMAP single and dual channel soil moisture retrievals. Geophysical Research Letters, 45(2), 758-765. https://doi: 10.1002/2017GL075656

Ferreira, L. and Duarte, D. 2019. Exploring the relationship between urban form, land surface temperature and vegetation indices in a subtropical megacity. Urban Climate, 27, 105-123. https://doi:10.1016/j.uclim.2018.11.002

Guha, S. and Govil, H. 2020. Land surface temperature and normalized difference vegetation index relationship: a seasonal study on a tropical city. SN Applied Sciences, 2(10), art 1661. https://doi:10.1007/s42452-020-03458-8

Hasnat, G. 2021. A time series analysis of forest cover and land surface temperature change over Dudpukuria-Dhopachari Wildlife Sanctuary using Landsat imagery. Frontiers in Forests and Global Change, 4, art 687988. https://doi.org/10.3389/ffgc.2021.687988(2021)

Kaur, R. and Pandey, P. 2020. Monitoring and spatio-temporal analysis of UHI effect for Mansa district of Punjab, India. Advances in Environmental Research, 9(1), 19-39.

Khandelwal, S., Goyal, R., Kaul, N. and Mathew, A. 2018. Assessment of land surface temperature variation due to change in elevation of area surrounding Jaipur, India. The Egyptian Journal of Remote Sensing and Space Science, 21(1), 87–94. https://doi.org/10.1016/j.ejrs. 2017.01.005

Kumari, B., Tayyab, M., Ahmed, I., Baig, M., Khan, M. and Rahman, A. 2022. Longitudinal study of land surface temperature (LST) using monoand split-window algorithms and its relationship with NDVI and NDBI over selected metro cities of India. Arab Journal of Geoscience, 13, 1–19. https://doi.org/doi: 10.1007/s12517- 020-06068-1.

Lein, J. 2011. Environmental Sensing: Analytical Techniques for Earth Observation. Chamberlin, Springer Science.

Macarof, P. and Statescu, F. 2017. Comparison of NDBI and NDVI as indicators of surface urban heat island effect in Landsat 8 imagery: A case study of Iasi. Present Environment and Sustainable Development, 11(2), 141-150. https://doi:10.1515/pesd-2017-0032

Malik, M. and Shukla, J. 2018. Retrieving of land surface temperature using thermal remote sensing and GIS techniques in Kandaihimmat Watershed, Hoshangabad, Madhya Pradesh. Journal of the Geological Society of India, 92(3), 298-304. https://doi:10.1007/s12594-018-1010-y

Mallick, J., Kant, Y. and Bharath, B. 2008. Estimation of land surface temperature over Delhi using Landsat-7 ETM+. Journal of Indian Geophysics Union, 12(3), 131–140.

Mustafa, E., Co, Y. and Liu, G. 2020. Study for predicting land surface temperature (LST) using Landsat data: A comparison of four algorithms. Advances in Civil Engineering, 2020, art 7363546. https://doi:10.1155/2020/7363546

Niclòs, R., Galve, J., Valiente, J., Estrela, M. and Coll, C. 2011. Accuracy assessment of land surface temperature retrievals from MSG2-SEVIRI data. Remote Sensing Environment, 115(8), 2126-2140. https://doi:10.1016/j.rse.2011.04.017

Orhan, O., Ekercin, S. and Dadaser-Celik F. 2014. Use of Landsat land surface temperature and vegetation indices for monitoring drought in the Salt Lake Basin area, Turkey. The Scientific World Journal, 2014, art 142939. https://doi:10.1155/2014/142939

Pal, S. and Ziaul, S. 2017. Detection of land use and land cover change and land surface temperature in English Bazar urban centre. The Egyptian Journal of Remote Sensing and Space Science, 20(1), 125-145. https://doi:10.1016/j.ejrs.2016.11.003

Pandey, A.K, Singh, S., Berwal, S., Kumar, D., Pandey, P., Prakash, A., Lodhi, N., Maithani, S., Jain, V.K. and Kumar, K. 2014. Spatio-temporal variations of urban heat island over Delhi. Urban Climate, 10(1), 119-133. doi:10.1016/j.uclim.2014.10.005

Qin, Z., Karnieli, A. and Berliner, P. 2022. A mono-window algorithm for retrieving land surface temperature from Landsat TM data and its application to the Israel-Egypt border region. International Journal of Remote Sensing, 22(18), 3719-3746. https://doi.org/10.1080/ 0143116001 0006971(2001)

Rahaman, S.N. and Shermin, N. 2021. Identifying built-up area expansion and comparing two conventional built-up area extraction methods from LANDSAT imagery: A case study on Khulna City. Academia Letters, 2021, art 758. https://doi.org/10.20935/al758

Ranagalage, M. 2017. An urban heat island study of the Colombo Metropolitan Area, Sri Lanka, based on Landsat data (1997–2017). International Journal of Geo-Information, 6, art 189. https://doi:10.3390/ijgi6070189

Sun, D., Pinker, R. and Basara, J. 2004. Land surface temperature estimation from the next generation of geostationary operational environmental satellites: GOES M–Q. Journal of Applied Meteorology, 43(2), 363-372. https://doi.org/10.1175/1520-0450(2004)043<0363:LSTEFT>2.0.CO;2

Weng, Q. 2009. Thermal infrared remote sensing for urban climate and environmental studies: Methods, applications, and trends. ISPRS Journal of Photogrammetry and Remote Sensing, 64(4), 335–344. https://doi.org/10.1016/j.isprsjprs.2009.03.007

Weng, Q., Lu, D. and Schubring, J. 2004. Estimation of land surface temperature–vegetation abundance relationship for urban heat island studies. Remote Sensing Environment, 89(4), 467-483. https://doi:10.1016/j.rse.2003.11.005

Xu, H. 2010. Analysis of impervious surface and its impact on urban heat environment using the Normalized Difference Impervious Surface Index (NDISI). Photogrammetric Engineering & Remote Sensing, 76(5), 557-565. https://doi:10.14358/pers.76.5.557

Yadav, S., Hashia, H. and Perwaiz, S. 2019. Urban built-up and leader in energy and environmental design (LEED) certification: A case study of National Capital Territory (NCT) of Delhi, India. Journal of Global Resources, 06(01), 81–88. https://doi.org/10.46587/ jgr.2019.v06i01.013

Yuan, F. and Bauer, M. 2007. Comparison of impervious surface area and normalized difference vegetation index as indicators of surface urban heat island effects in Landsat imagery. Remote Sensing Environment, 106(3), 375-386. https://doi:10.1016/j.rse.2006.09.003

Zha, Y., Gao, J. and Ni, S. 2003. Use of normalized difference built-up index in automatically mapping urban areas from TM imagery. International Journal of Remote Sensing, 24(3), 583–594. https://doi.org/10.1080/01431160304987

Zheng, Y., Tang, L. and Wang, H. 2021. An improved approach for monitoring urban built-up areas by combining NPP-VIIRS nighttime light, NDVI, NDWI, and NDBI. Journal of Cleaner Production, 328, art 129488. https://doi.org/10.1016/j.jclepro.2021.129488

Zhu, L., Cho, D., Jeon, C. and Lee, S. 2016. Evaluating methods for extracting built-up area using NPP-VIIRS night time light data and local spatial statistics. Journal of the Korean Urban Geographical Society, 19(3), 145-163. https://doi:10.21189/jkugs.19.3.11

Received:9th December 2022
Accepted:1st April 2023